

# Advances in Screen Printing of Conductive Nanomaterials for Stretchable Electronics

Nathan Zavanelli and Woon-Hong Yeo\*



Cite This: *ACS Omega* 2021, 6, 9344–9351



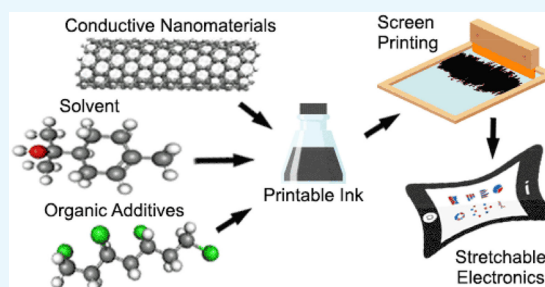
Read Online

ACCESS |

Metrics & More

Article Recommendations

**ABSTRACT:** Stretchable electronics have demonstrated tremendous potential in wearable healthcare, advanced diagnostics, soft robotics, and persistent human–machine interfaces. Still, their applicability is limited by a reliance on low-throughput, high-cost fabrication methods. Traditional MEMS/NEMS metallization and off-contact direct-printing methods are not suitable at scale. In contrast, screen printing is a high-throughput, mature printing method. The recent development of conductive nanomaterial inks that are intrinsically stretchable provides an exciting opportunity for scalable fabrication of stretchable electronics. The design of screen-printed inks is constrained by strict rheological requirements during printing, substrate–ink attraction, and nanomaterial properties that determine dispersibility and percolation threshold. Here, this review provides a concise overview of these key constraints and a recent attempt to meet them. We begin with a description of the fluid dynamics governing screen printing, deduce from these properties the optimal ink rheological properties, and then describe how nanomaterials, solvents, binders, and rheological agents are combined to produce high-performing inks. Although this review emphasizes conductive interconnections, these methods are highly applicable to sensing, insulating, photovoltaic, and semiconducting materials. Finally, we conclude with a discussion on the future opportunities and challenges in screen-printing stretchable electronics and their broader applicability.



## 1. INTRODUCTION

Biological surfaces can stretch and deform. Their mechanics differ greatly from rigid systems, and this mechanical mismatch causes traditional electronic systems to interface very poorly with human skin.<sup>1</sup> As a result, wearable healthcare applications were limited for many years to obtrusive systems that coupled incompletely with the body.<sup>1</sup> Stretchable electronics, on the other hand, can integrate with a variety of soft materials, offering a high degree of control over their material properties.<sup>1</sup> Central to these systems are electrical interconnections that are highly conductive and maintain their structural integrity with strain.<sup>2</sup> Traditionally, these interconnects consist of ultrathin metals with fractal geometries that are fabricated through established MEMS/NEMS methods.<sup>1</sup> This method offers excellent control over print architecture and high spatial resolution, but it is expensive and low throughput.<sup>1</sup> In contrast, conductive nanomaterials can be directly patterned on substrates through noncontact techniques, like aerosol jet, inkjet, and electrohydrodynamic (EHD) printing, and contact methods, like gravure, flexographic, and screen printing.<sup>2</sup> However, each of these approaches presents several challenges.<sup>2</sup> Aerosol jet printing offers good print resolution and thin material deposition, but it is too low-throughput for industrial scales.<sup>2</sup> Inkjet printing is sufficiently scalable, but clogging at the nozzle head limits the use of large particles and high viscosities are required in a printable ink.<sup>2</sup>

EHD printing overcomes several of these limitations by pulling inks to the substrate with electrical forces, allowing the formation of high-resolution traces through a large nozzle. However, it is limited by a low yield rate and strict stand-off height requirements.<sup>2</sup> Contact printing methods are a high-throughput and mature alternative, and among these approaches, screen printing offers the highest control over pattern deposition, print resolution, and substrate choice.<sup>2,3</sup>

Several essential manufacturing requirements must be met to fabricate stretchable printed circuit boards (PCBs) via screen printing.<sup>4</sup> First, the conductive ink must be printable on the stretchable target substrate.<sup>1</sup> This requires the ink's rheology to be optimized for the complicated fluid dynamics during screen printing and the surface chemistry at the ink–mesh and ink–substrate interface suitable to the printing mechanisms described in section 2.<sup>5,6</sup> Second, the ink must be highly conductive and maintain this conductivity with strain up to 20% for wearable applications.<sup>2</sup> This requires a solid

Received: February 3, 2021

Accepted: March 22, 2021

Published: March 31, 2021



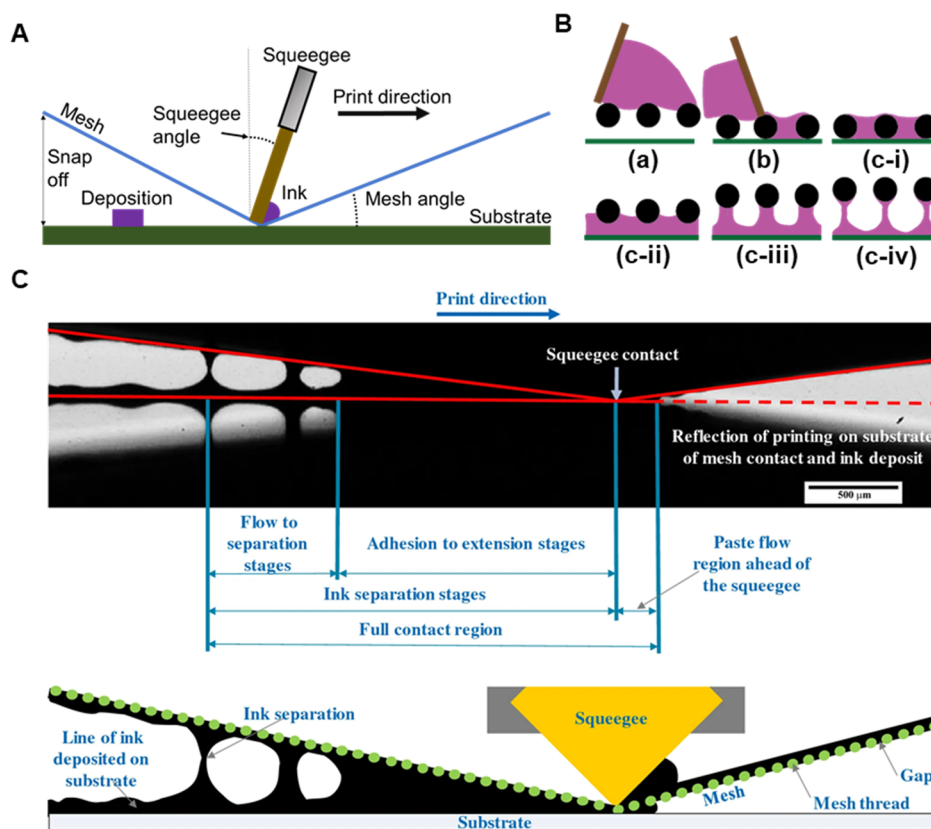


**Figure 1.** Overview of screen printing techniques. (A) Depiction of the ink transfer process during screen printing from screen to a substrate. (B) Schematic showing the three stages of screen printing, as proposed by Abbott et al.<sup>6</sup> (a) Excess fluid on the mesh after flood stroke. (b) Squeegee forces the screen into contact with the substrate and fills cavities with ink. (c) (i–iv) Screen separates from the substrate, and ink is pulled from mesh. (C) High-speed image and illustration of the final stage involved in ink transfer (reprinted with permission from *J. Coat. Technol.* **2020**, *17*, 447–459.<sup>7</sup> Copyright 2020, Springer).

understanding of the nanomaterial–polymer matrix interactions that form the material’s percolation threshold.<sup>5–7</sup> Third, the resulting print must be durable through repeated strain over multiple uses, which is also controlled primarily by the particle dispersion and matrix composition.<sup>2</sup> Finally, the print width should be sufficiently thin ( $<100\ \mu\text{m}$ ) and precisely controlled to allow for reliable and small feature device fabrication.<sup>1,2</sup> This is a function of the ink rheology, interface surface chemistry, and screen-printing fabrication parameters.<sup>6,8</sup>

These fundamental requirements are nontrivial to meet, necessitating the discovery of new nanomaterial–polymer formulations.<sup>2</sup> Although microscale materials have been proposed, the large, asymmetric particles lead to decreased pseudoplasticity caused by interparticle attractions and durability concerns due to fragmentation with cyclic strain.<sup>9</sup> Likewise, polymer inks, like those formed from PEDOT:PSS, are highly stretchable and transparent, but they are limited by high sheet resistance.<sup>10</sup> In contrast, recent advancements in the formulation of nanomaterial inks comprising nanoparticles (NP), nanowires (NW), or nanotubes (NT) embedded in a stretchable polymer matrix offer an exciting new approach to screen printing stretchable conductors.<sup>2</sup> Screen-printable stretchable inks may be formulated by many additional materials (e.g., graphene, graphene oxide, nanographene platelets, and liquid metals). However, we focus here on NPs, NWs, and NTs, because they exhibit the most satisfactory mechanics, electrical behavior, and dispersibility.<sup>2,4,9,11,12</sup> For

each of these materials, finely controlling material properties and interparticle interactions during synthesis, particle dispersion, and polymer matrix composition allows for the delivery of high printability, conductivity, reliability, and resolution in a printable ink.<sup>5,7,12</sup>

In this review, we summarize nanomaterial approaches to screen printing stretchable electronics, with a particular focus on the optimization of nanomaterial properties, polymer matrix composition, particle dispersion, surface chemistry, and screen-printing manufacturing parameters to address the key design criteria in fabricating stretchable PCBs. We begin with an overview of the screen-printing process and fluid mechanics, which informs our discussion of print parameters and ink rheology optimization. We then discuss the specific chemical mechanisms employed in each nanomaterial’s dispersion and the formulation of this material into a printable ink. We continue with a summary of state-of-the-art screen-printed nanomaterial interconnects and conclude with commentary on the future development and critical challenges facing the field.

## 2. SCREEN PRINTING FUNDAMENTALS

**2.1. Ink Transfer Mechanics.** Screen printing involves the direct contact transfer of ink from a stenciled mesh to a target substrate, as shown in Figure 1A.<sup>8</sup> As an ancient art, screen printing has long been implemented in garment manufacturing without understanding the scientific principles that govern it.<sup>6,13</sup> In addition, the first analytic models describing the process made several deceptively intuitive assumptions that

proved to be incorrect, and their poor predictive power further fueled the idea that screen printing was an art, not a science.<sup>6,13,14</sup> Riemer et al. first implemented the Navier–Stokes equation in cylindrical polar coordinates simplified for creeping flows as an analytic model to describe the ink transfer during screen printing, but they neglected the effects of ink adhesive and cohesive forces, instead implicitly assuming that ink is injected out of mesh openings solely by hydrostatic pressure.<sup>13</sup> As a result, the proposed model did not produce realistic flows or accurately predict thick film depositions.<sup>13</sup> The assumption that ink is forced out of the mesh openings and onto the substrate via downward force is intuitive but not correct.<sup>14</sup> Instead, Messerschmitt et al. argued that the ink's adhesion primarily guides screen printing to the mesh and substrate and its cohesive forces, and Abbott et al. developed this qualitative theory into a computational model that could be experimentally validated.<sup>6,14</sup> They based this model on Messerschmitt's three-stage printing mechanism, represented by (a), (b), and (c) in Figure 1B.<sup>6</sup> In Figure 1B (a), the ink is flooded into the mesh such that it occupies the entire open area.<sup>6</sup> In Figure 1B (b), the mesh is brought into contact with the substrate via downward force from the substrate.<sup>6</sup> The ink adheres to both the substrate and the mesh based on the interface free energy for each system.<sup>6</sup> In Figure 1B (c), the mesh is pulled vertically, and the ink forms filament structures until its cohesive forces are overcome, leading to a deposition of ink on the substrate and a percentage remaining in the mesh.<sup>6</sup> This final stage can be divided into four substages (c-i, ii, iii, iv).<sup>6</sup> First, (c-i) is the *adhesion* of the ink to the substrate and mesh; second, (c-ii) is the *extension* of the ink structure as the mesh is pulled vertically; third, (c-iii) is the *flow* of ink into filament structure; and fourth, (c-iv) is the *separation* of the two ink structures.<sup>6</sup> These distinct stages can be captured with high-speed imaging, as shown in Figure 1C.<sup>7</sup>

Clearly, any process guided by these steps will be predominantly influenced by the ink viscosity, cohesive and adhesive forces, pseudoplasticity, and mesh angle relative to the substrate, not the squeegee pressure and speed, and these parameters will be discussed in the next section.<sup>6</sup> In their computational model, Abbott et al. divided the ink volume between the mesh and the substrate into 100 rectangular sections in two dimensions and calculated the capillary number and meniscus behavior based on the ink's rheology, adhesive and cohesive forces, squeegee speed and pressure, mesh height, angle, and threads per micron.<sup>6</sup> Numerical integration yielded the theoretical ink remaining in the mesh, and thus the printed thickness.<sup>6</sup> Even though this model is two-dimensional and neglects substrate properties, ink compression, and inertia effects, it correlated well with experimental results.<sup>6</sup> Although further studies have shown that the complicated variable interactions make the proper determination of specific parameters like print height and width challenging, Abbott's qualitative assertions have largely formed the basis for subsequent investigations into print parameter and ink property optimization.<sup>8</sup>

**2.2. Key Process Parameters and Ink Properties.** The deposition height is determined by the percentage of ink remaining in the mesh during extension and filament separation. The resolution is guided by the ink–substrate equilibrium contact angle and ink pseudoplasticity. The print quality is determined primarily by minimizing filament size, assuming the process is set up correctly to proceed in the four steps described previously.<sup>5,6,8</sup> This is because large filaments

produce thick circular depositions in the area where they collapse, leading to an uneven print and reduced resolution.<sup>6</sup> The deposition height has been shown to depend very little on the squeegee speed and pressure; instead, it is highly dependent on the mesh geometry and, to a lesser degree, the ink composition and interaction with the substrate.<sup>5,6,8</sup> This thickness depends on the substrate's ability to pull ink from the mesh, and thus increases approximately linearly with the fraction of open area in the mesh.<sup>11</sup> It is also dependent on the ink's cohesive forces and adhesion to the substrate.<sup>7,8</sup> Viscosity was not found to impact print height to a high degree, but increasing ink cohesion (e.g., higher material loading or polymer composition) and higher substrate–ink adhesion do.<sup>8</sup> For ultrathin prints, the height is also dependent on the print resolution, where the equilibrium contact angle causes the ink to slump down to the side and lower the print.<sup>5</sup> This slumping is the primary limiting factor in print resolution, and thus print resolution and height are inversely related.<sup>8</sup> Therefore, decreasing the mesh open area increases resolution, but this also impacts the printability of the ink by increasing adhesive forces, especially with large material loading.<sup>11</sup> In addition, the mesh can be chemically treated to control adhesion, the substrate surface chemistry can be modified to increase the contact angle, the ink can be made thicker and more viscous, the humidity can be minimized, and the substrate reduced in temperature.<sup>5,6,8,12</sup> Nanomaterial screen printing inks are constrained by the demands of printability, conductivity, and stretchability. Still, the development of ultrathin (<70  $\mu\text{m}$ , or the resolution limit of microscale flake inks) screen printing depositions is an area of active research.<sup>4,11</sup> Recent work has focused on improving ink viscosity, viscosity recovery time, yield stress and ink–substrate adhesion through careful choice of particle solvent and rheological agents, resulting in print resolutions down to 22  $\mu\text{m}$ .<sup>4,11,12,15</sup> For instance, dispersion agents are necessary to prevent particle agglomeration, but they greatly decrease viscosity, and several solvents, like ethyl cellulose, have consistently demonstrated promising rheological properties.<sup>12</sup> Finally, print quality depends on a complex interaction of manufacturing parameters and ink properties, but the device settings can be easily optimized due to the speed of prototyping.<sup>8</sup> Therefore, printable ink design that also demonstrates high conductivity with strain and minimum printable resolution form the central challenge.<sup>12</sup> An ink's printability depends primarily on several rheological parameters.<sup>5</sup> Ideal screen-printing inks are pseudoplastic, meaning they decrease viscosity with shear, but they are neither viscoelastic nor thixotropic.<sup>6</sup> Pseudoplasticity allows the ink to flow from the mesh when shear is applied during extension, then rapidly recover during separation to yield a high-resolution trace.<sup>6</sup> Pseudoplasticity is controlled primarily by the choice and concentration of polymer binders and rheological additives, although particle dispersion, geometry, and loading also play an essential role.<sup>12</sup> For instance, hydroxypropyl methyl cellulose (HMC) was found to greatly increase printability in AgNW inks through both increased pseudoplasticity and improved dispersion stability due to bonding between hydroxyl groups and the surface of AgNWs.<sup>4</sup> Similarly, ethyl cellulose was found to improve pseudoplasticity in low concentrations compared to Thixatrol in a systematic study and validated in a carbon-based nanomaterial conductive ink with excellent printability and resolution.<sup>11,12</sup> Beyond pseudoplasticity, viscoelasticity and thixotropicity tend to reduce print quality and should be minimized.<sup>6</sup> Viscoelastic

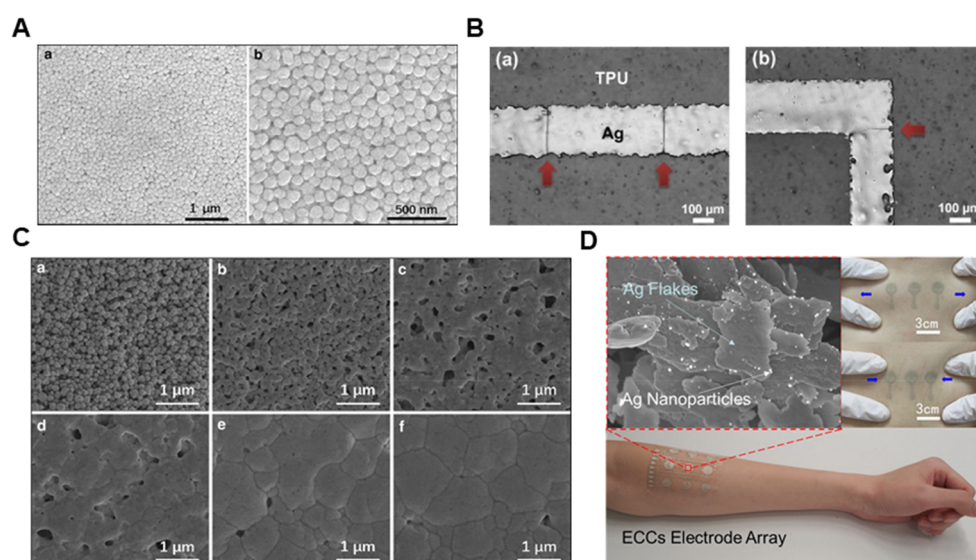


**Figure 2.** Silver Nanoparticles (AgNPs) for stretchable screen-printed electronics. (A) SEM images of printed AgNPs (reproduced with permission from *J. Mater. Sci. Mater.* **2017**, *28* (22), 16939–16947.<sup>16</sup> Copyright 2020, Springer). (B) Optical micrograph images of pattern fracturing after applied strain (reproduced with permission from *J. Manuf. Process.* **2014**, *120*, 216–220.<sup>9</sup> Copyright 2014, Elsevier). (C) AgNPs after sintering at different temperature for 30 min: (a) without sintering, (b) 220 °C, (c) 240 °C, (d) 260 °C, (e) 280 °C, and (f) 300 °C (reproduced with permission from *J. Mater. Sci. Mater.* **2017**, *28* (22), 16939–16947.<sup>16</sup> Copyright 2020, Springer). (D) SEM image of in situ formed AgNPs and photos of their application for a stretchable screen-printed ECG array (reprinted with permission from *ACS Appl. Mater. Interfaces.* **2019**, *11*, 8567–8575.<sup>18</sup> Copyright 2019, ACS. photograph courtesy of Wei Guo, copyright 2019).

**Table 1.** Reported Conductivity and Stretchability of Screen-Printed Conductors Using Nanomaterials

ref	conductor	substrate	material loading (wt %)	primary solvent	sintering	conductivity	stretchability
9	AgNP	PU	73	terpineol	60 min at 150 °C	$3.3 \times 10^4$ (S/cm)	8%
16	AgNP	PI	80	HMC	30 min at 220 °C	$1.2 \times 10^5$ (S/cm)	
17	AgNP	PU	75	tetradecane	room temperature	1.97 Ω/sq	~38%
4	AgNW	PUA (transfer from PET)	6.6	HMC	15 min at 150 °C	$4.67 \times 10^4$ (S/cm)	~70%
20	AgNW	PDMS	2	terpineol	photonic (laser 0.67 ms, 9 W)	1.9 Ω/sq	~20%
21	AgNW	PDMS	70	terpineol	2 h at 80 °C	$6.9 \times 10^4$ (S/cm)	~100%
24	MWCNT	silicone	7.5	ethanol	room temperature	0.5–1.3 Ω/sq	
25	Ag/MWCNT	PI	0.6 (CNT)	not mentioned, added SDS	20 min at 120 °C	7.26 μΩ/sq	

inks tend to prolong filament formation and result in uneven or otherwise damaged prints.<sup>5,6,12</sup> Thixotropic inks cause a time delay in the pseudoplastic viscosity recovery with low strain, resulting in slumping and poor print quality.<sup>6</sup> Finally, parameters like viscosity, yield stress, and surface tension tend to be interrelated because of their dependence on cohesive forces in the ink, but these parameters have contradictory impacts on printability.<sup>4,6</sup> Therefore, an optimal condition that is low viscosity to permit fine print resolution, high in yield stress to improve postprint recovery, and high in surface tension to maximize contact angle is desired.<sup>5,6,12</sup>

### 3. NANOMATERIAL INK APPROACHES

**3.1. Fundamentals.** Conductive screen-printing inks generally consist of three components: conductive nano- or microparticles, organic binders and rheological agents, and a solvent.<sup>4,5,12</sup> These inks' formation depends heavily on the chemical and geometrical properties of the conductive materials and rheological requirements covered previously.<sup>4,5</sup> In choosing a conductive filler, the tendency to agglomerate, percolation threshold, and particle size are key design

criteria.<sup>9,15</sup> Strong intermolecular forces leading to agglomeration complicate dispersion, high percolation thresholds require heavy material loading, limiting printability and stretchability, and large particle sizes cause complications in fine trace width prints and can lead to fracturing.<sup>9</sup> Generally, the solvent is highly polar and the filler nonpolar.<sup>12</sup> This allows for an amphiphilic dispersion agent, like polyvinylpyrrolidone (PVP), to bind to the filler and create repulsive complexes that disperse throughout the matrix.<sup>9,12</sup> However, PVP greatly degrades printability in large concentrations because of its tendency to produce low viscosity and non-pseudo-plastic rheology.<sup>4</sup> As discussed previously, the solvent, binder, and rheological agents are crucial in determining printability, and many potential combinations exist to impart the proper rheology.<sup>5</sup>

**3.2. Silver Nanoparticle (AgNP) Inks.** Spherical AgNPs, like those shown in Figure 2A, have been frequently investigated for screen-printing applications despite several key material properties that are not conducive to proper ink design.<sup>9,16,17</sup> First, strong interparticle attractions tend to agglomerate particles, complicating dispersion.<sup>9,17</sup> Second,

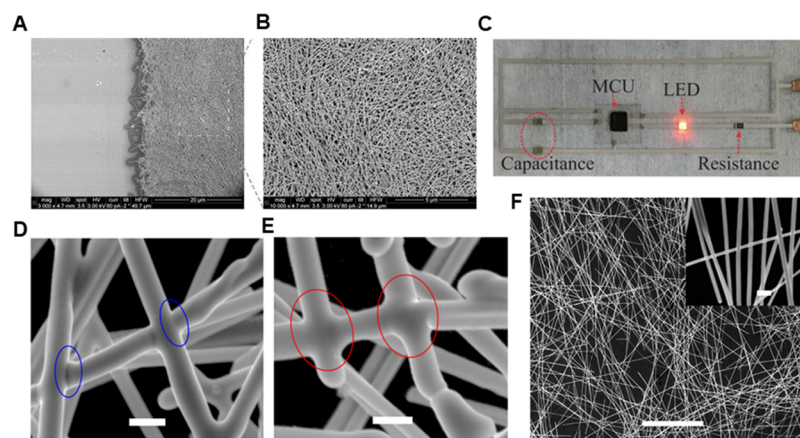


**Figure 3.** Silver nanowires (AgNWs) for stretchable screen-printed electronics. (A,B) SEM images of screen-printed AgNWs after post-treatment with low (A) and high (B) magnification (reproduced with permission from *Adv. Mater.* **2016**, *28*, 5986–5996.<sup>4</sup> Copyright 2016, Wiley). (C) Functional circuit composed of stretchable AgNW interconnects on PDMS (reprinted with permission from *J. Semicond.* **2018**, *39* (1), 015002.<sup>21</sup> Copyright 2018, IOP Press). (D–F) SEM images depicting (D,E) laser welded AgNWs with 100 nm scale bars and (F) AgNW network with 10  $\mu\text{m}$  scale bars (reproduced with permission from *npj Flex. Electron.* **2019**, *3* (13).<sup>20</sup> Copyright 2019, Springer Nature).

despite these attractive forces, the spherical geometry results in a high percolation threshold without sintering.<sup>17</sup> Finally, the AgNPs tend to form gaps when stretched or fracture when sintered.<sup>9</sup> Examples of fractured AgNP prints after strain is shown in Figure 2B, and Figure 2C depicts sintered AgNP patterns, which appear as semirigid films.<sup>9,16</sup>

These material properties present several critical challenges to be overcome. Because AgNPs are difficult to disperse, mechanisms to limit PVP concentrations, typically through removal, additional surfactants, or dissolution in acetone, are required.<sup>9</sup> The high percolation threshold requires substantial material loading, which further complicates dispersion and limits options to improve printability.<sup>9,17</sup> Finally, trade-offs exist between conductivity and reliability with strain when using AgNPs. Despite these challenges, several groups have achieved promising ink formulations within the material constraints. For instance, Jung et al. dissolved AgNPs with high material loading in  $\alpha$ -terpineol to yield bulk conductivity above  $3 \times 10^5$  S/cm but noted conductivity degradation beyond 8% strain.<sup>9</sup> On the other hand, Kim et al. optimized the AgNP dispersion for stretchability with minimal material loading and sintering, leading to consistent conductivity up to 38% strain, but only 1.97  $\Omega/\text{sq}$  bulk conductivity.<sup>9,17</sup> These results are contextualized with the remaining works to be discussed in Table 1. AgNPs can also be formed in situ from Ag flake fillers, as shown in Figure 2D.<sup>18</sup> These inks have demonstrated high conductivity ( $>1 \times 10^5$  S/cm) and stretchability (80% strain), but they are limited in resolution because of large particles, which can also lead to fracture.<sup>18</sup> Although AgNPs were the first nanomaterial explored for screen printing conductive inks, these limitations and trade-offs have ultimately required the investigation of additional materials when high conductivity, stretchability, and reliability are required simultaneously.<sup>4</sup>

**3.3. Silver Nanowire (AgNW) Inks.** AgNWs are particularly attractive as a conductive basis for screen printing applications because their elongated geometry imparts several key advantages over spherical NPs.<sup>2,4,20,21</sup> When dispersed in random orientations, the long particles form highly conductive networks, as shown in Figure 3A–B, maintaining contact during strain to a much higher degree than NPs.<sup>4</sup> In addition, NWs are sufficiently thin to allow for low material loading

without fracture or loss of conductivity, which greatly improves printability and resolution when combined with optimized solvents and additives.<sup>4,21</sup> Finally, NWs tend to disperse much more easily than NPs, requiring much fewer stabilizing additives that degrade printability, like PVP.<sup>4,19</sup> Qibing et al. were the first to demonstrate the full potential of AgNWs by designing an ink with high conductivity ( $4.7 \times 10^5$  S/cm), stretchability (100% strain), reliability (cyclic bending, 1000 cycles), and resolution (50  $\mu\text{m}$ ).<sup>4</sup> These results were achieved through the use HMC as a dispersion agent, Zonyl FS-300 as a surface tension modifier, and very low material loading (6.6%) for optimal pseudo plastic recovery after printing.<sup>4</sup> The process did, however, require the transfer of printed traces from a flexible poly(ethylene terephthalate) (PET) substrate to poly(urethane acrylate) (PUA), reducing scalability.<sup>4</sup> Likewise, Cui et al. used a similar transfer approach with PDMS to design highly conductive circuit interconnects with 100% stretchability and excellent reliability: an application in Figure 3C.<sup>21</sup> Finally, Shamim et al. directly printed AgNWs on an ultraviolet/ozone (UVO) treated PDMS substrate by utilizing low material loadings and a 6 wt % ethyl cellulose/PVP-terpineol ink matrix.<sup>20</sup> The low material loading resulted in a transparent deposition, but it greatly limited conductivity (41  $\Omega/\text{sq}$ ) and stretchability ( $<20\%$ ) compared to other works.<sup>4,20</sup> To address these trade-offs, the AgNW deposition was laser sintered post-print with a 9 W Yb:fiber laser and exposure time of 0.67 ms to yield AgNW nanowelding, as shown in Figure 3D.<sup>20</sup> The result increased conductivity from 41 to 1.9  $\Omega/\text{sq}$  with no change in stretchability or reliability. The final nanowelded network is shown in Figure 3F.<sup>20</sup> These prints have demonstrated sufficient conductivity, stretchability, and reliability (1000 rounds cyclic testing) for use in wearable applications, but no study of high-resolution patterning was conducted.<sup>20</sup> In addition, it is unknown whether similar methods can be employed with higher material loadings to yield conductivities approaching that of intrinsic silver.<sup>20</sup>

**3.4. Carbon Nanotube (CNT) Inks.** CNTs are a versatile, low-cost material with excellent elastic and conductive properties, and their high aspect ratio is promising for stretchable conductor applications; however, CNTs interact strongly through van der Waals forces and tend to agglomerate into heterogeneous distributions.<sup>22–24</sup> Typically, sufficient

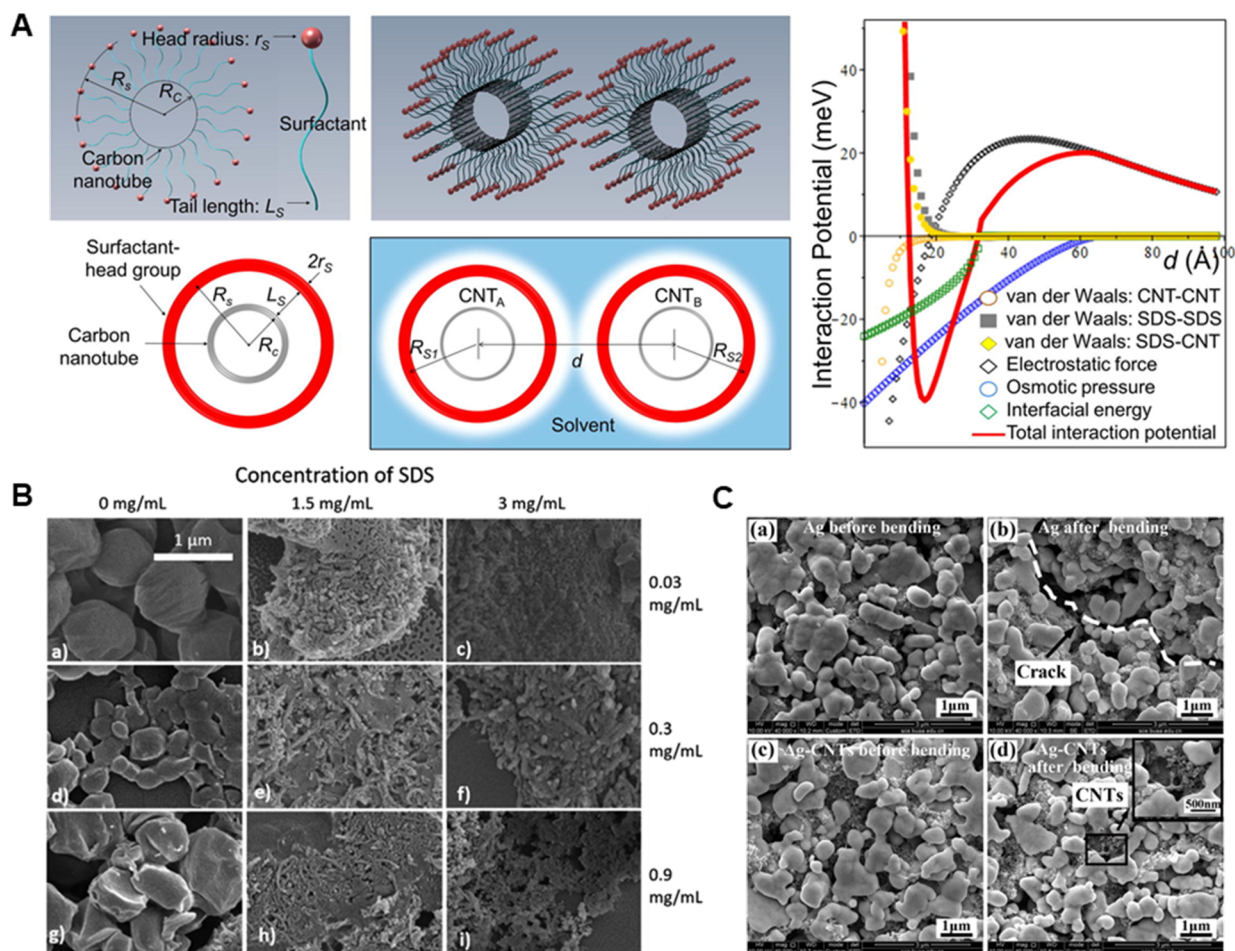


**Figure 4.** Carbon nanotubes (CNTs) for stretchable screen-printed electronics. (A) Mean-density model of surfactant heads for the dispersion of CNTs with sodium dodecyl sulfate (SDS) with an analytically derived potential of mean force for SDS coverage of 70% (reproduced with permission from *Appl. Surf. Sci.* **2018**, 439, 1133–1142.<sup>22</sup> Copyright 2018, Elsevier). (B) SEM images of CNT dispersion with varying concentrations of SDS and CNTs, reproduced with permission from *RSC Adv.* **2018**, 8 (30), 16444–16454.<sup>23</sup> Copyright 2018, The Royal Chemical Society). (C) SEM images of printed Ag (a, b) and Ag-CNTs (c, d) before bending (a, c) and after (b, d) 1000-cycle bending ( $r = 4$  mm), reprinted with permission from *J. Mater. Sci. Technol.* **2017**, 33 (10), 1113–1119.<sup>25</sup> Copyright 2017, Elsevier).

dispersions require the addition of anionic surfactants, like sodium dodecyl sulfate (SDS).<sup>23</sup> SDS is strongly amphiphilic, like PVP, allowing it to bind to the hydrophobic CNT surfaces and dissolve in water.<sup>23</sup> The negatively charged SDS tails create repulsive forces, greatly aiding in dispersion.<sup>22</sup> Figure 4A depicts the analytically derived interaction potential for 70% SDS coverage on CNTs, demonstrating a suitable profile for dispersion.<sup>22</sup> The analytic model predicted that dispersion effectiveness and solution mechanics are very sensitive to SDS coverage percentage, and this hypothesis has been validated in numerous experiments, such as the one depicted in Figure 4B.<sup>23</sup> Stringent dispersion requirements complicate the design of stretchable, conductive, and printable inks, but such inks have been reported.<sup>24</sup> Surendran et al. demonstrated a printable multiwalled CNT (MWCT) ink for screen printing using 9 wt % material loading, 7.5% SDS–ethanol dispersant loading, and 50 wt % PVP concentration.<sup>24</sup> The solution was mechanically agitated to promote dispersion. Because of high PVP concentration, viscosity was low, but the ink was screen-printable on a variety of substrates. No discussion of the resolution was provided, but it is assumed that low viscosity would preclude resolutions below 100  $\mu\text{m}$ . Likewise, there is no discussion of conductivity during strain, but the sheet

resistance with three printing passes was reported as 0.5  $\Omega/\text{sq}$ .<sup>24</sup> Because proper CNT dispersions are difficult to design, CNTs are typically employed in sensor applications (beyond the scope of this review) that take advantage of their remarkable material properties or as secondary fillers to improve Ag microparticle inks.<sup>2,22,25</sup> Deng et al. compared the electrical and mechanical properties of Ag inks with particle sizes of around 0.2–1  $\mu\text{m}$  before and after the addition of CNTs.<sup>25</sup> The CNTs formed conductive bridges between microparticles, as shown in Figure 4C, that improved conductivity by more than 60% and demonstrated excellent reliability during cyclic bending and thermal shock.<sup>25</sup> However, this approach is limited by the difficulty of dispersing CNTs and assembling bridge structures in a highly printable ink, and no discussion of resolution is provided.<sup>25</sup> Overall, CNTs are highly promising materials for screen printing stretchable conductors, but novel approaches to overcome particle agglomeration require further investigation.

#### 4. CONCLUSIONS

Screen printing of nanomaterial conductors presents one possible mechanism by which tremendous advances in stretchable electronics can be translated to medical and

commercial applications that directly improve patient outcomes and quality of life.<sup>2</sup> Central to such applications are inks with nanomaterial, solvent, binder, and rheological agent solutions tailored specifically to screen printing's fluid dynamics and maintenance of conductivity with strain.<sup>5–8</sup> An ink's effectiveness is primarily limited by the nanomaterial filler's properties (e.g., interaction potential and geometry) that determine dispersibility and conductive network formation. However, substantial opportunities remain to improve solvent and additive compositions, especially in the case of CNT inks.<sup>4,5,24</sup> Although AgNPs were the first nanomaterial considered for screen printing and remain a common filler choice, particle agglomeration limits dispersion, and high percolation thresholds require high material loading.<sup>9</sup> AgNWs overcome these challenges through an elongated geometry that promotes conductive network formation at low material loadings, allowing for substantial freedom in ink rheological optimization.<sup>4</sup> In the short term, further investigations into AgNW ink dispersion techniques, rheology, and sintering will likely make them the material of choice for screen-printed stretchable conductors, despite their high cost.<sup>4</sup> CNTs, however, present both the greatest promise and technical challenges, making them a strong target for future development.<sup>24</sup> Excellent elastic and electrical properties and cost-effective production make them highly suitable for screen printing, but powerful interparticle attractions make stable dispersion difficult.<sup>24</sup> Overall, screen printing is a promising method for stretchable interconnect fabrication, but substantial investigations into particle dispersion, ink rheology, pattern mechanics under strain, and conductive network formation remain before it can translate stretchable electronics from laboratory to commercial and medical use.

## AUTHOR INFORMATION

### Corresponding Author

**Woon-Hong Yeo** – *George W. Woodruff School of Mechanical Engineering, Center for Human-Centric Interfaces and Engineering at the Institute for Electronics and Nanotechnology, Wallace H. Coulter Department of Biomedical Engineering, and Parker H. Petit Institute for Bioengineering and Biosciences, Neural Engineering Center, Institute for Materials, Institute for Robotics and Intelligent Machines, Georgia Institute of Technology, Atlanta, Georgia 30332, United States; [orcid.org/0000-0002-5526-3882](https://orcid.org/0000-0002-5526-3882); Phone: +1-404-385-5710; Email: [whyeo@gatech.edu](mailto:whyeo@gatech.edu); Fax: +1-404-894-1658*

### Author

**Nathan Zavanelli** – *George W. Woodruff School of Mechanical Engineering, Center for Human-Centric Interfaces and Engineering at the Institute for Electronics and Nanotechnology, Georgia Institute of Technology, Atlanta, Georgia 30332, United States*

Complete contact information is available at:  
<https://pubs.acs.org/10.1021/acsoomega.1c00638>

### Notes

The authors declare no competing financial interest.

## Biographies



Dr. Woon-Hong Yeo is an Assistant Professor in the George W. Woodruff School of Mechanical Engineering and the Wallace H. Coulter Department of Biomedical Engineering, and the Director of the Center for Human-Centric Interfaces and Engineering at Georgia Institute of Technology. He received his PhD in mechanical engineering at the University of Washington, Seattle, in 2011. From 2011–2013, he worked as a postdoctoral research fellow at the Beckman Institute and Frederick Seitz Materials Research Center at the University of Illinois at Urbana–Champaign. His research areas include soft electronics, human–machine interfaces, nanobiosensors, and soft robotics.



Mr. Nathan Zavanelli is currently a PhD student in the George W. Woodruff School of Mechanical Engineering at the Georgia Institute of Technology. He received his B.S. degree in Electrical Engineering from the Georgia Institute of Technology in 2019. His work is at the intersection of soft electronics, signal processing, machine learning, and human physiology. He studies fully printed methods for high throughput fabrication of wearable devices with soft device mechanics optimized for signal transduction from the body.

## ACKNOWLEDGMENTS

We acknowledge the support by the National Science Foundation (grant NRI-2024742) and the IEN Center Grant from the Georgia Tech Institute for Electronics and Nanotechnology.

## REFERENCES

- (1) Jeong, J. W.; Yeo, W. H.; Akhtar, A.; Norton, J. J.; Kwack, Y. J.; Li, S.; Jung, S. Y.; Su, Y.; Lee, W.; Xia, J.; Cheng, H.; Huang, Y.; Choi, W. S.; Bretl, T.; Rogers, J. A. Materials and optimized designs for human-machine interfaces via epidermal electronics. *Adv. Mater.* **2013**, *25* (47), 6839–46.

- (2) Huang, Q.; Zhu, Y. Printing Conductive Nanomaterials for Flexible and Stretchable Electronics: A Review of Materials, Processes, and Applications. *Adv. Mater. Technol.* **2019**, *4*, 1800546.
- (3) Goldoni, R.; Ozkan-Aydin, Y.; Kim, Y. S.; Kim, J.; Zavanelli, N.; Mahmood, M.; Liu, B.; Hammond, F. L., 3rd; Goldman, D. I.; Yeo, W. H. Stretchable Nanocomposite Sensors, Nanomembrane Interconnectors, and Wireless Electronics toward Feedback-Loop Control of a Soft Earthworm Robot. *ACS Appl. Mater. Interfaces* **2020**, *12* (39), 43388–43397.
- (4) Liang, J.; Tong, K.; Pei, Q. A Water-Based Silver-Nanowire Screen-Print Ink for the Fabrication of Stretchable Conductors and Wearable Thin-Film Transistors. *Adv. Mater.* **2016**, *28*, 5986–5996.
- (5) Reinhardt, K.; Hofmann, N.; Eberstein, M. The importance of shear thinning, thixotropic and viscoelastic properties of thick film pastes to predict effects on printing performance. *2017 21st European Microelectronics and Packaging Conference (EMPC) & Exhibition 2017*, 1–7.
- (6) Kapur, N.; Abbott, S. J.; Dolden, E. D.; Gaskell, P. H. Predicting the behavior of screen printing. *IEEE Trans. Compon., Packag., Manuf. Technol.* **2013**, *3*, 508–515.
- (7) Potts, S. J.; Phillips, C.; Jewell, E.; Clifford, B.; Lau, Y. C.; Claypole, T. High-speed imaging the effect of snap-off distance and squeegee speed on the ink transfer mechanism of screen-printed carbon pastes. *J. Coat. Technol. Res.* **2020**, *17*, 447–459.
- (8) Philip, B.; Jewell, E.; Greenwood, P.; Weirman, C. Material and process optimization screen printing carbon graphite pastes for mass production of heating elements. *J. Manuf. Process* **2016**, *22*, 185–191.
- (9) Kim, K. S.; Jung, K. H.; Jung, S. B. Design and fabrication of screen-printed silver circuits for stretchable electronics. *Microelectron. Eng.* **2014**, *120*, 216–220.
- (10) Tseghai, G. B.; Malengier, B.; Fante, K. A.; Nigusse, A. B.; Van Langenhove, L. Development of a flex and stretchy conductive cotton fabric via flat screen printing of PEDOT:PSS/PDMS conductive polymer composite. *Sensors* **2020**, *20*, 1742.
- (11) Hyun, W. J.; Secor, E. B.; Hersam, M. C.; Frisbie, C. D.; Francis, L. F. High-resolution patterning of graphene by screen printing with a silicon stencil for highly flexible printed electronics. *Adv. Mater.* **2015**, *27*, 109–115.
- (12) Xu, C.; Willenbacher, N. How rheological properties affect fine-line screen printing of pastes: a combined rheological and high-speed video imaging study. *J. Coat. Technol.* **2018**, *15*, 1401–1412.
- (13) Riemer, D. The Theoretical Fundamentals of the Screen-Printing Process. *Microelectron. Int.* **1989**, *6* (1), 8–17.
- (14) Messerschmitt, E. Rheological Considerations for Screen Printing Inks. *Screen Print* **1982**, *72* (10), 62–65.
- (15) Hyun, W. J.; Lim, S.; Ahn, B. Y.; Lewis, J. A.; Frisbie, C. D.; Francis, L. F. Screen Printing of Highly Loaded Silver Inks on Plastic Substrates Using Silicon Stencils. *ACS Appl. Mater. Interfaces* **2015**, *7* (23), 12619–24.
- (16) Wang, Z.; Liang, X.; Zhao, T.; Hu, Y.; Zhu, P.; Sun, R. Facile synthesis of monodisperse silver nanoparticles for screen printing conductive inks. *J. Mater. Sci.: Mater. Electron.* **2017**, *28* (22), 16939–16947.
- (17) Yoon, S.; Kim, H. K. Cost-effective stretchable Ag nanoparticles electrodes fabrication by screen printing for wearable strain sensors. *Surf. Coat. Technol.* **2020**, *384*, 125308.
- (18) Guo, W.; Zheng, P.; Huang, X.; Zhuo, H.; Wu, Y.; Yin, Z.; Li, Z.; Wu, H. Matrix-Independent Highly Conductive Composites for Electrodes and Interconnects in Stretchable Electronics. *ACS Appl. Mater. Interfaces* **2019**, *11*, 8567–8575.
- (19) He, X.; He, R.; Lan, Q.; Wu, W.; Duan, F.; Xiao, J.; Zhang, M.; Zeng, Q.; Wu, J.; Liu, J. Screen-printed fabrication of PEDOT: PSS/silver nanowire composite films for transparent heaters. *Materials* **2017**, *10*, 220.
- (20) Li, W.; Yang, S.; Shamim, A. Screen printing of silver nanowires: balancing conductivity with transparency while maintaining flexibility and stretchability. *npj Flex. Electron.* **2019**, *3*, 1.
- (21) Yuan, W.; Wu, X.; Gu, W.; Lin, J.; Cui, Z. Printed stretchable circuit on soft elastic substrate for wearable application. *J. Semicond.* **2018**, *39*, 015002.
- (22) Joung, Y. S. A mean-density model of ionic surfactants for the dispersion of carbon nanotubes in aqueous solutions. *Appl. Surf. Sci.* **2018**, *439*, 1133–1142.
- (23) Niezabitowska, E.; Smith, J.; Prestly, M. R.; Akhtar, R.; von Aulock, F. W.; Lavalley, Y.; Ali-Boucetta, H.; McDonald, T. O. Facile production of nanocomposites of carbon nanotubes and polycaprolactone with high aspect ratios with potential applications in drug delivery. *RSC Adv.* **2018**, *8* (30), 16444–16454.
- (24) Menon, H.; Aiswarya, R.; Surendran, K. P. Screen printable MWCNT inks for printed electronics. *RSC Adv.* **2017**, *7* (70), 44076–44081.
- (25) Hu, D.; Zhu, W.; Peng, Y.; Shen, S.; Deng, Y. Flexible carbon nanotube-enriched silver electrode films with high electrical conductivity and reliability prepared by facile screen printing. *J. Mater. Sci. Technol.* **2017**, *33* (10), 1113–1119.